The structural models for the $(2\sqrt{3} \times 2\sqrt{3})R30^{\circ}$ reconstructions of 3C-SiC(111) and 6H-SiC(0001) surfaces

2006 J. Phys.: Condens. Matter 18 6953

(http://iopscience.iop.org/0953-8984/18/30/001)

INSTITUTE OF PHYSICS PUBLISHING JOURNAL OF PHYSICS: CONDENSED MATTER

J. Phys.: Condens. Matter **18** (2006) 6953–6963 doi:10.1088/0953-8984/18/30/001

The structural models for the $(2\sqrt{3} \times 2\sqrt{3})$R30° reconstructions of 3C-SiC(111) and 6H-SiC(0001) surfaces

Yun Li, Xun Wang and Ling Ye

Surface Physics Laboratory, Fudan University, Shanghai 200433, People's Republic of China

E-mail: yun_lee@126.com

Received 28 March 2006, in final form 23 May 2006
Published 14 July 2006
Online at stacks.iop.org/JPhysCM/18/6953

Abstract

We propose a double-trimer model and a single-trimer model for $(2\sqrt{3} \times 2\sqrt{3})$R30° reconstructions observed on the surface of the 3C-SiC(111) island and the 6H-SiC(0001) surface, respectively. We study their atomic and electronic structures by using first principles calculations within density-functional theory. The total energy calculations indicate that the double-trimer model and the single-trimer model are energetically more favourable than the previously reported DV model and Tri-Ad model, respectively. The simulated scanning tunnelling microscopic images for these two models agree fairly well with the experimental observations. The surface energy band structures of the single-trimer model and the Tri-Ad model were compared, which might provide a criterion for the further discrimination of the exact models by experimental evaluation.

(Some figures in this article are in colour only in the electronic version)

1. Introduction

It is known that the surface structures of silicon carbide (SiC) strongly depend on the crystalline orientations, the stoichiometry and the growth conditions. Different sample preparation conditions often give rise to different structures of the same reconstruction, e.g. the symmetric and asymmetric bridging-dimer models of the C-terminated SiC(001)-c(2 × 2) reconstruction and the alternatively up and down dimer model and the missing-row asymmetric dimer model of the Si-terminated SiC(001)-c(4 × 2) reconstruction [1].

Recently, two different structures of the $(2\sqrt{3} \times 2\sqrt{3})$R30° reconstruction were also observed on the 3C-SiC(111) and 6H-SiC(0001) surfaces [2–4]. Pascual *et al* [2] first reported the observation of the $(2\sqrt{3} \times 2\sqrt{3})$R30° reconstruction on the surface of the 3C-SiC(111) island formed by heat reaction of the Si(111)-(7 × 7) substrate with the fullerene molecules.

They found that the scanning tunnelling microscopic (STM) images of this reconstruction were bias dependent. In the empty-state STM image under low bias voltage two trimer-like protrusions with different heights appeared in each $(2\sqrt{3} \times 2\sqrt{3})$ cell, and this $(2\sqrt{3} \times 2\sqrt{3})$ periodicity would be converted into (2×2) under a very high positive sample bias voltage. But in the filled-state STM image a dark Y-shape appeared in each $(2\sqrt{3} \times 2\sqrt{3})$ cell. In addition, they also observed that the $(2\sqrt{3} \times 2\sqrt{3})$ phase always coexisted with the (3×3) phase over the annealing temperature of 1100 °C and only the $(2\sqrt{3} \times 2\sqrt{3})$ phase remained at the annealing temperature of 850 °C. This implies that the Si coverage of the $(2\sqrt{3} \times 2\sqrt{3})$ reconstruction is higher than that of the (3×3) reconstruction on the surface of the 3C-SiC(111) island.

However, Amy *et al* [4] observed another $(2\sqrt{3} \times 2\sqrt{3})$ phase which was prepared by annealing the 6H-SiC(0001)-(3×3) surface at 900 °C without Si flux. In their experiment, only one big protrusion appeared in each $(2\sqrt{3} \times 2\sqrt{3})$ cell in both filled-state and empty-state STM images. These STM behaviours are quite different from those on the surface of the 3C-SiC(111) island. In addition, this $(2\sqrt{3} \times 2\sqrt{3})$ phase always coexisted with the (3×3) phase at the annealing temperature of 900 °C, and long time annealing could reduce the area of the (3×3) phase but it never vanished. Therefore, Amy *et al* claimed that in their experiment the Si coverage of the $(2\sqrt{3} \times 2\sqrt{3})$ reconstruction is slightly lower than that of the (3×3) reconstruction and the $(2\sqrt{3} \times 2\sqrt{3})$ reconstructions observed by them and by Pascual *et al* have different structures.

For the $(2\sqrt{3} \times 2\sqrt{3})$ reconstruction observed on the 3C-SiC(111) island, Yang *et al* proposed a 'demisemi vacancy (DV)' model, in which 1/4 monolayer of Si vacancies are sitting in the topmost layer of the Si-terminated SiC substrate [3]. The electronic structure of this model was further investigated by Peng *et al* [5], using the density functional theory calculation within a cluster model. As mentioned above, the $(2\sqrt{3} \times 2\sqrt{3})$ phase on the 3C-SiC(111) island has a higher Si coverage than the (3×3) phase, which has a Si-adatom coverage of 13/9 for the Starke model [6] or 12/9 for the fluctuant-trimer (FT) model [7]. In the DV model, however, the Si-adatom coverage is $-4/12$. The large discrepancy of the Si-adatom coverage could actually rule out the DV model. For the $(2\sqrt{3} \times 2\sqrt{3})$ reconstruction observed on the 6H-SiC(0001) surface, Amy *et al* proposed a Tri-Ad structural model, in which nine Si atoms and three vacancies form the lowest adlayer on the Si termination of the SiC substrate and another four Si atoms form a tetrahedron on the adlayer [4]. This model was actually derived from the (3×3) reconstruction model proposed by Starke *et al* [6] by reducing the Si-adatom coverage from 13/9 to 13/12. A very noticeable characteristic of the Tri-Ad model is 1/4 monolayer of Si vacancies in the lowest adlayer. Previous studies of the SiC(0001)-(3×3) reconstruction showed that the vacancies in the adlayer could remarkably increase the formation energy of the surface [6, 8, 9]. Therefore, it is reasonable to consider whether there is a more stable structural model for the $(2\sqrt{3} \times 2\sqrt{3})$ reconstruction observed by Amy *et al*.

In our work, first we proposed a double-trimer model and a single-trimer model for the $(2\sqrt{3} \times 2\sqrt{3})$R30° reconstructions observed on the surface of the 3C-SiC(111) island and the 6H-SiC(0001) surface, respectively, and then we discussed their surface atomic and electronic structures. Basing on the calculated surface charge distributions, we simulated the STM images of these two models and compared them with the data of previous STM experiments. Finally the stabilities of these two models and previously reported DV and Tri-Ad models were compared.

2. Calculation models and method

The first principles calculations were preformed within the framework of density-functional theory (DFT). To perform the computations we used the Vienna *ab initio* simulation package described in [10]. The generalized-gradient approximation (GGA) proposed by Wang and

Perdew [11] was employed for evaluating the exchange–correlation energy. Vanderbilt-type ultrasoft pseudopotentials [12] were used to describe the electron–ion interactions and the wavefunctions were expanded by a plane wave basis set with the energy cut-off of about 21 Ryd. The $(2\sqrt{3} \times 2\sqrt{3})$ surfaces were modelled in the supercells. Each supercell consists of a slab of six SiC bilayers and a vacuum of 16 Å, which is thick enough to isolate the interactions between adjacent slabs. The C atoms in the C termination of the slab were saturated with hydrogen atoms in order to get rid of dangling bonds. Additional Si adatoms were placed on the clean surface to cover the Si termination of the slab. A grid of 3×3 **k** points was used to sample the surface Brillouin zone. These computational parameters are sufficient to give well converged results for the total energy and the electronic structure calculations. The six SiC bilayers were placed at their ideal bulk positions and then the atoms in the half slab containing Si adatoms were allowed to relax until the Hellman–Feynman forces on these atoms vanished within 1 meV Å^{-1}.

3. Results and discussion

For the 3C-SiC(111)-$(2\sqrt{3} \times 2\sqrt{3})$ reconstruction, the structural model proposed in this work is shown in figure 1. In this model, each $(2\sqrt{3} \times 2\sqrt{3})$ cell contains 18 Si adatoms. Twelve of them form a vacancy-free adlayer on the Si termination of the SiC substrate and the others form two trimers with different heights on the adlayer. In figure 5, we show the structural model of the 6H-SiC(0001)-$(2\sqrt{3} \times 2\sqrt{3})$ reconstruction, in which 12 Si atoms are located in the vacancy-free adlayer and the other three Si atoms form a trimer on the adlayer. We named them the double-trimer (DT) model and the single-trimer (ST) model, respectively. Actually, the DT model has a Si-adatom coverage of 18/12, which is higher than that of the (3×3) reconstruction as required by the experiments of Pascual *et al* [2], while the ST model has a Si-adatom coverage of 15/12, which is slightly lower than that of the (3×3) reconstruction as required by the experiments of Amy *et al* [4]. For comparison, the total energies and electronic structures of all structural models of the $(2\sqrt{3} \times 2\sqrt{3})$ reconstruction were calculated.

3.1. Atomic and electronic structures of 3C-SiC(111)-$(2\sqrt{3} \times 2\sqrt{3})$-R30° surface

The relaxation calculation gave the optimized $(2\sqrt{3} \times 2\sqrt{3})$ surface atomic structure of the DT model shown in figure 1. The heights of atoms (relative to the Si-terminated atoms of the SiC substrate), bond lengths and bond angles are listed in table 1. In the DT model, the Si atoms *a*, *b*, and *c* in the first adlayer have no lateral displacement. The distance between atom *a* and the underneath substrate Si atom almost equals the bond length of Si atoms in the bulk, while atoms *b* and *c* relax downward 0.14 Å and upward 0.41 Å, respectively. The bond angles listed in table 1 indicate that the bonding configurations of atoms *a* and *b* are close to $sp^2 + p$, while that of atom *c* is close to asymmetric sp^3. Large lateral displacements lead to highly asymmetric sp^3 bonding configurations of atoms *d*, *e* and *f*.

In the second adlayer, three equivalent atoms *g* form trimer I and the other three equivalent atoms *h* form trimer II. Trimer II is 0.73 Å higher than trimer I. A remarkable feature is that atom *g* and its neighbouring atom *h* form a buckled Si dimer. The bond length of the dimer is 2.4 Å and the buckling angle is 17.7°, as shown in figure 1(c). This configuration of three dimers with threefold symmetry on SiC surface has never been found before. Similar to the buckled dimer on the Si(100)-p(2×1) surface [13–17], the dangling bonds of two dimer atoms *g* and *h* in the DT model also form a π bond, which leads to a semiconducting surface.

The bond angles listed in table 1 suggest that the three back-bonds of atom *g* consist of asymmetric hybridized sp^3 orbitals, while those of atom *h* mostly consist of p orbitals. So the

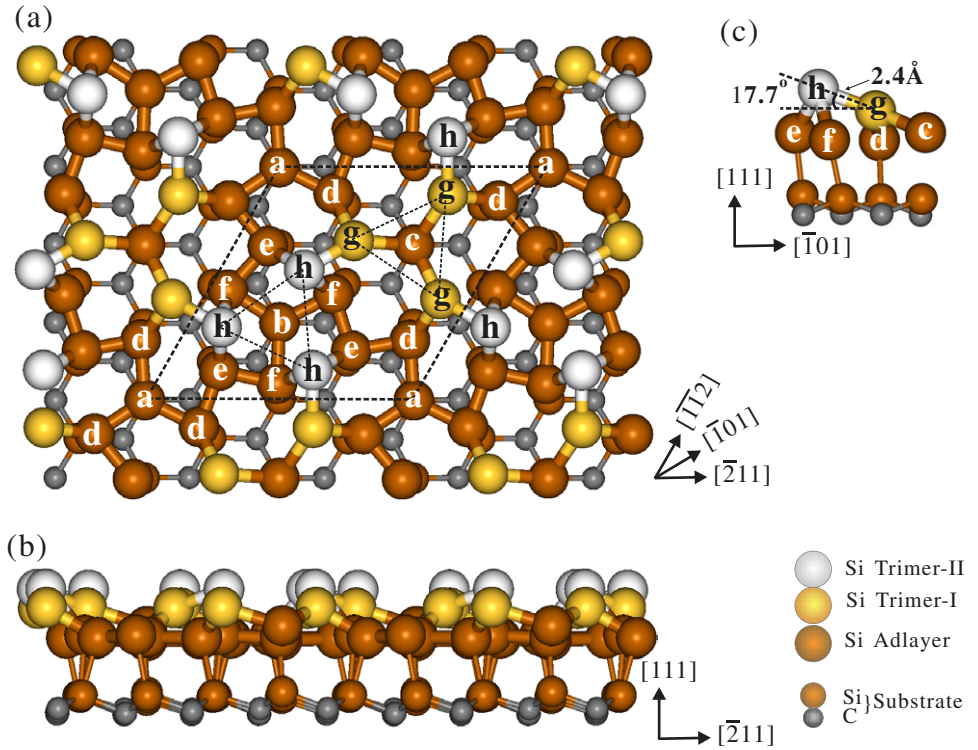

Figure 1. Schematic diagrams of the DT model for the 3C-SiC(111)-($2\sqrt{3} \times 2\sqrt{3}$) reconstruction: (a) top view, (b) side view, and (c) buckled dimer. Equivalent Si atoms on the surface are denoted by the same character.

Table 1. Heights (relative to the Si-terminated atoms of SiC substrate), bond angles, and bond lengths of surface Si atoms in the 3C-SiC(1111)-($2\sqrt{3} \times 2\sqrt{3}$) DT model.

Atom height	(Å)	Bond length	(Å)	Bond angle	(deg)
a	2.33	*ad*	2.39	*dad*	120.0
b	2.21	*bf*	2.42	*fbf*	120.0
c	2.76	*cg*	2.51	*gcg*	112.0
d	2.31	*de*	2.35	*cgd*	103.2
e	2.41	*dg*	2.35	*dgh*	105.0
f	2.28	*ef*	2.34	*hgc*	147.2
g	3.49	*eh*	2.50	*ehf*	81.5
h	4.22	*fh*	2.46	*fhg*	64.0
		gh	2.40	*ghe*	94.5

dangling bond of atom *g* consists of an asymmetric sp^3 orbital, while that of atom *h* mostly consists of an s orbital. These two kinds of dangling bonds induce two surface states in the bandgap of SiC bulk. Because of the absence of dangling bonds, the surface state densities of other adatoms are very small. As shown in figure 2, the s-like dangling-bond state of atom *h* lies a little above the valence band maximum (VBM) of SiC bulk, while the sp^3-like dangling-bond state of atom *g* overlaps with the conduction band minimum (CBM) of SiC bulk. In addition, a part of the surface state of atom *g* is filled and overlaps with the filled state of atom *h*, and

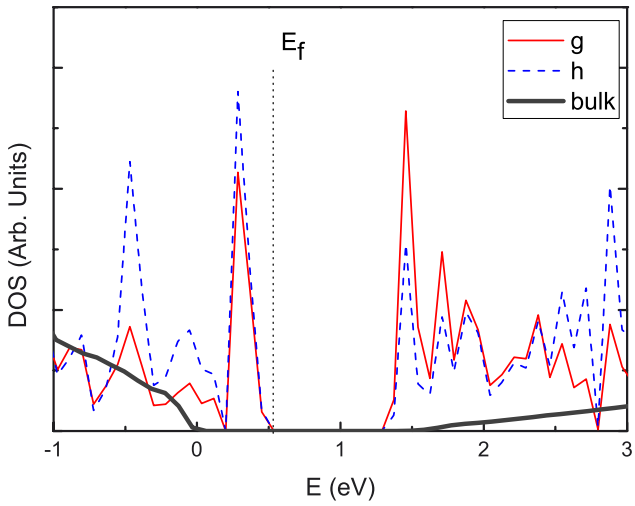

Figure 2. The local DOSs of atoms g and h in the DT model for the 3C-SiC(111)-$(2\sqrt{3} \times 2\sqrt{3})$ reconstruction. As a reference, the DOS of SiC bulk is also plotted and the valence band maximum of SiC bulk is taken as energy zero.

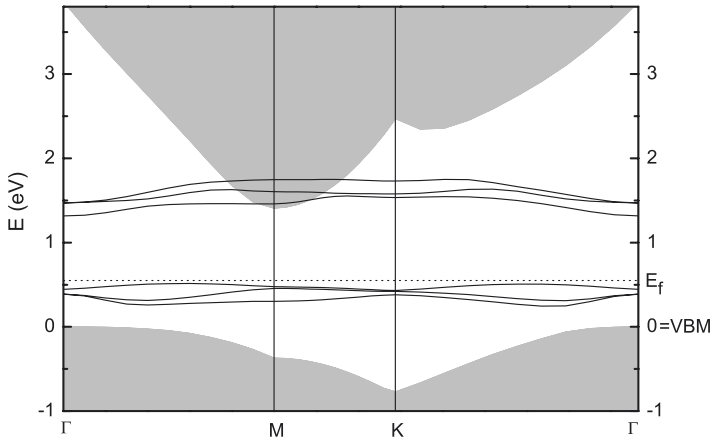

Figure 3. Surface energy band structure of the DT model for the 3C-SiC(111)-$(2\sqrt{3} \times 2\sqrt{3})$ reconstruction. Only those energy levels deriving from the dangling bonds are plotted. The projected bulk band structure is shown as shaded regions. The VBM of SiC bulk is taken as energy zero. For simplicity, the detailed structures in valence and conduction bands are omitted.

similarly a part of the surface state of atom h is empty and overlaps with the empty state of atom g. This suggests that the dangling bonds of atoms g and h form a π bond. Obviously, the dangling bond of atom h possesses more charge than that of atom g.

The calculated energy band structure of the DT model is shown in figure 3. In the projected bulk bandgap, three filled levels and three empty levels correspond to the bonding states and the anti-bonding states formed by the dangling bonds of three dimers in each $(2\sqrt{3} \times 2\sqrt{3})$ cell, respectively. These bonding states and anti-bonding states form two subbands with bandwidth of 0.3 eV respectively. The filled π band is 0.2 eV above the bulk VBM, and the empty π^* band overlaps with the bulk CBM. The gap between π and π^* bands is 0.85 eV. It should be

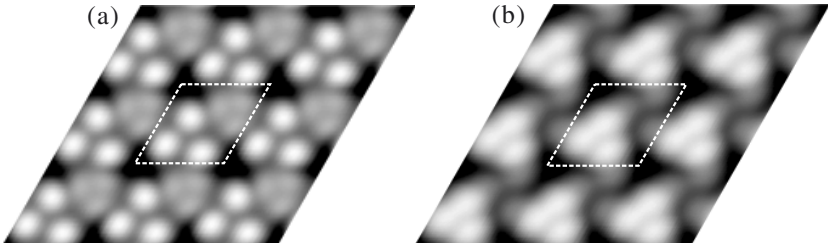

Figure 4. Simulated STM images of the DT model for the 3C-SiC(111)-$(2\sqrt{3} \times 2\sqrt{3})$ reconstruction: (a) empty-state image ($V_s = +1.5$ V), and (b) filled-state image ($V_s = -0.8$ V). The $(2\sqrt{3} \times 2\sqrt{3})$ cell is marked by dashed lines.

noted that, comparing with the experimental value, the local density approximation calculation usually underestimates the bandgap by about 30% [18].

Based on the calculated surface charge distributions, we simulated STM images of the DT model by using the Bardeen approach [19] and the Tersoff–Hamann [20] model of the STM tip. In the simulated empty-state image shown in figure 4(a), each $(2\sqrt{3} \times 2\sqrt{3})$ cell includes three bright spots and three less bright spots which originate from the dangling bonds of the trimer-II atoms *h* and trimer-I atoms *g*, respectively. This trimer feature of the STM image was revealed in the experiments of Pascual *et al* clearly [2], but cannot be deduced from the DV model. In the simulated filled-state image shown in figure 4(b), the spots on trimer I become darker than those in the empty-state STM image. The reason is that the empty surface state density of atom *g* is larger than that of atoms *h*, but the filled surface state density of atoms *g* is smaller than that of atoms *h*. Moreover, the dark areas on atom *a* and its three neighbouring atoms *d*, and a part of the dark areas on atoms *g*, form a threefold dark Y-shape area. The above simulated empty-state and filled-state STM images agree fairly well with the experimental STM images [2, 3].

3.2. Atomic and electronic structures of the 6H-SiC(0001)-$(2\sqrt{3} \times 2\sqrt{3})R30^\circ$ surface

Figure 5 shows the optimized structure of the ST model, in which one Si trimer sits on the top of the vacancy-free adlayer. Table 2 lists the heights, bond lengths and bond angles of the atoms on the surface. The bond angles indicate that the bonding configurations of atoms *a*, *b* and *c* are close to $sp^2 + p$, and those of atoms *d* and *f* correspond to asymmetrical $sp^2 + p$. Only atoms *e* and *g* have a dangling bond each, and their bonding configurations are remarkably different. The bond angles indicate that the three back-bonds of atom *e* mostly consist of p orbitals, so the dangling bond has more s orbital, whereas for atom *g* the dangling bond has more p orbital because the configurations of the three back-bonds are close to asymmetric sp^3. These two kinds of dangling bond also induce two surface states in the bandgap of SiC bulk, as shown in figure 6. The dangling-bond state of atom *e* lies below that of atom *g*. The surface state of atom *e* is almost filled, while most of the surface state of atom *g* is empty. This implies that most of the charge in the dangling bonds of atom *g* transfers into those of atom *e*, which could remarkably lower the surface energy.

The calculated surface energy band structure of the ST model is shown in figure 7(a). In the bandgap of SiC bulk, there are three filled dangling-bond levels mainly contributed from the dangling bonds of atoms *e* and three empty levels mainly from the dangling bonds of atoms *g*. The Fermi level is located in the gap between these surface energy bands, which indicates that the surface of the ST model is semiconducting. We also calculated the surface energy band

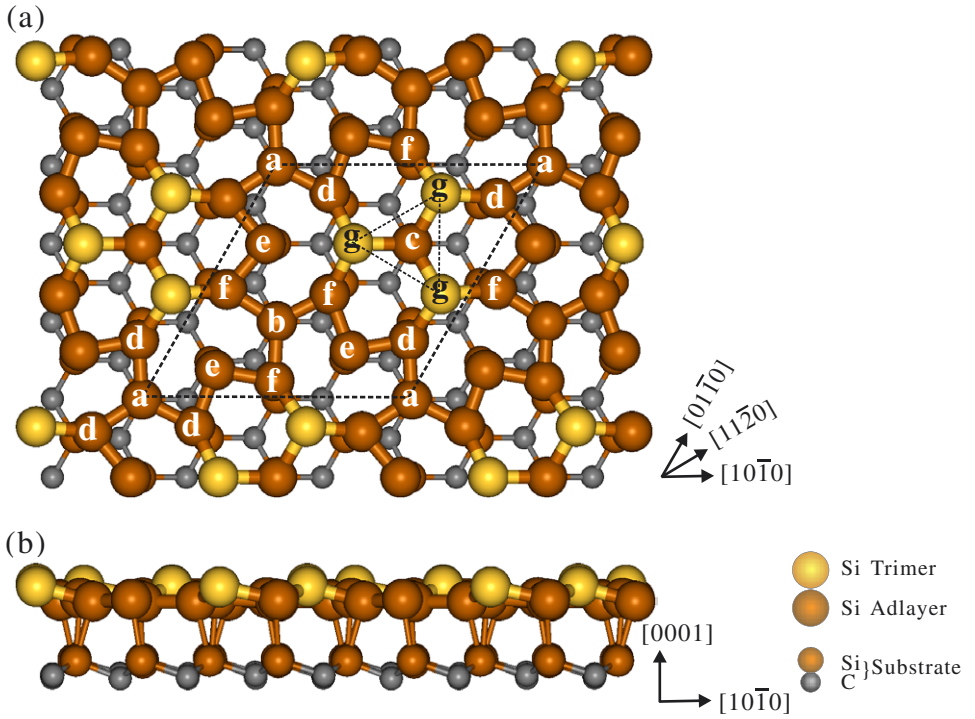

Figure 5. Schematic diagrams of the ST model for the 6H-SiC(0001)-($2\sqrt{3}\times 2\sqrt{3}$) reconstruction: (a) top view; (b) side view. Equivalent Si atoms on the surface are denoted by the same character.

Table 2. Heights (relative to the Si-terminated atoms of the SiC substrate), bond angles, and bond lengths of surface Si atoms in the 6H-SiC(0001)-($2\sqrt{3}\times 2\sqrt{3}$) ST model. ($e'$ corresponds to the atom beneath atom e.)

Atom height	(Å)	Bond length	(Å)	Bond angle	(deg.)
a	2.32	ad	2.35	dad	120.0
b	2.32	bf	2.35	fbf	120.0
c	2.43	cg	2.37	gcg	115.7
d	2.35	de	2.37	dee'	93.6
e	2.44	dg	2.29	fee'	93.7
f	2.34	ef	2.37	def	99.5
g	2.93	fg	2.29	cgd	110.2
				dgf	122.7
				fgc	110.6

structure of the Tri-Ad model as shown in figure 7(b), which is very different from that of the ST model. The Fermi level of the Tri-Ad model lies in the middle of a surface state, therefore the surface of the Tri-Ad model is metallic. This significant difference of surface energy band structures between the ST model and the Tri-Ad model provides a convenient criterion for photoemission or other experiments distinguishing which model could be more appropriate for the ($2\sqrt{3}\times 2\sqrt{3}$) reconstruction observed by Amy *et al*.

For the ST model, the simulated STM images are shown in figure 8. In both filled-state and empty-state images, each ($2\sqrt{3}\times 2\sqrt{3}$) cell contains only one big bright spot. This is in

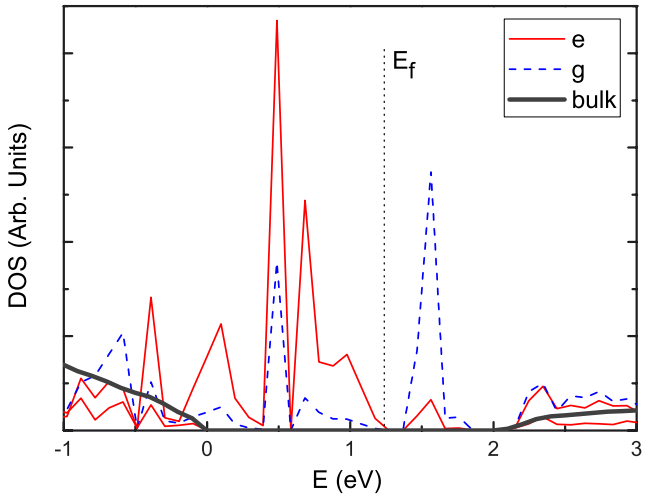

Figure 6. The local DOSs of atoms e and g in the ST model for the 6H-SiC(0001)-$(2\sqrt{3} \times 2\sqrt{3})$ reconstruction. As a reference, the DOS of SiC bulk is also plotted and the VBM of SiC bulk is taken as energy zero.

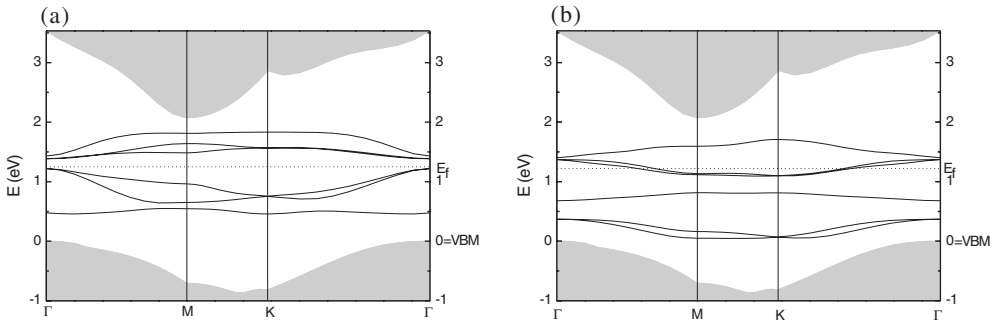

Figure 7. Surface energy band structure of the 6H-SiC(0001)-$(2\sqrt{3} \times 2\sqrt{3})$ reconstruction. (a) ST model, and (b) Tri-Ad model. Only those energy levels derived from the dangling bonds are plotted. The projected bulk band structure is shown as shaded regions. The VBM of SiC bulk is taken as energy zero. For simplicity, the detailed structures in valence and conduction bands are omitted.

agreement with the experimental STM images observed by Amy *et al* [4]. Another valuable observation in their experiment is the coexistence of the $(2\sqrt{3} \times 2\sqrt{3})$ phase and the (3×3) phase on the 6H-SiC(0001) surface. They found these two reconstruction domains have almost the same heights on the surface because the domain of the (3×3) phase is brighter than that of the $(2\sqrt{3} \times 2\sqrt{3})$ phase in the filled-state image but darker in the empty-state image. In our previous work, we have proposed another structural model of the SiC(0001)-(3×3) reconstruction, named the fluctuant trimer (FT) model. It consists of a vacancy-free Si adlayer on the Si termination of the SiC substrate and a Si trimer on the adlayer. The maximum height difference of three trimer-Si atoms is about 0.9 Å. This model is much better than the Starke model in terms of matching the experimental data of the x-ray diffraction Patterson map, direct and inverse photoemission spectroscopy, electron energy loss spectroscopy and STM [7]. We have also simulated STM images for the FT model under the same simulation parameters as those for the ST model, and compared their brightness in both filled-state and empty-state

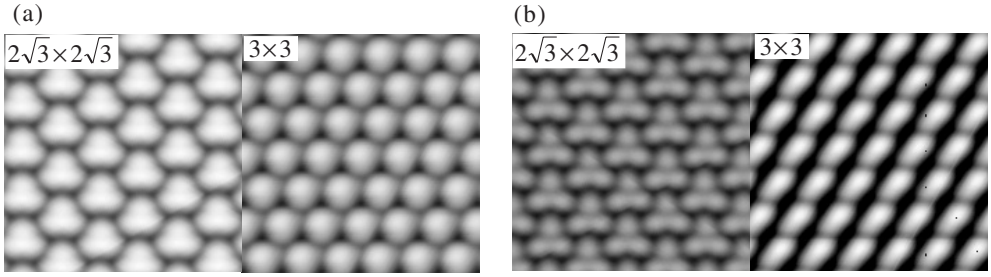

Figure 8. Simulated STM images of the $(2\sqrt{3}\times2\sqrt{3})$ phase of the ST model and the (3×3) phase of the FT model coexist on the 6H-SiC(0001) surface. (a) Empty-state images ($V_s = +1$ V), and (b) filled-state images ($V_s = -1.4$ V).

images. As shown in figure 8, the results basically agree with the above mentioned experimental features. For the $(2\sqrt{3}\times2\sqrt{3})$ reconstruction of the ST model, in the simulated filled-state STM image the bright spots are mainly contributed from the dangling-bond state of atoms *e*, while in the empty-state STM image they are contributed from the dangling-bond state of atoms *g*. In the (3×3) reconstruction of the FT model, the highest atom of the Si trimer is 0.9 Å higher than the lowest one. In addition, the dangling-bond state of the highest atom is filled, while that of the lowest one is empty [7]. Therefore, the simulated STM images of the coexisting surface of the $(2\sqrt{3}\times2\sqrt{3})$ and the (3×3) phases appear to be dependent on the bias polarity. Comparing with the $(2\sqrt{3}\times2\sqrt{3})$ phase, the spots of the (3×3) phase appear brighter in the filled-state image while in the empty-state image they become darker.

3.3. Stabilities of different structural models of the $(2\sqrt{3}\times2\sqrt{3})R30^\circ$ *reconstruction*

To compare the stabilities of different reconstruction models, we evaluated the formation energies of the DT, ST, DV, and Tri-Ad models using the expression suggested by Qian *et al* [21] and Northrup *et al* [22]. The results are shown in figure 9, where $\mu_{\mathrm{Si(bulk)}}$ is the chemical potential of bulk Si atoms and ΔH_f is the formation heat of SiC bulk. In our calculation ΔH_f is 0.56 eV per pair, which is very close to the value of 0.51 eV calculated by Sabisch *et al* but smaller than the experimental value of 0.72 eV per pair [23]. Our calculations show that the total energies of all the above $(2\sqrt{3}\times2\sqrt{3})$ models do not depend on the polytypes of the 3C-SiC and the 6H-SiC substrates. The energy difference of the same model on the above two SiC substrates is actually within the calculation limit of 4 meV per (1×1) cell, which is negligible for the purpose in the present study. For convenience, the formation energies of all structural models for the $(2\sqrt{3}\times2\sqrt{3})$ reconstructions on the above two SiC substrates are plotted in the same figure. One can see that for the 3C-SiC(111) surface the formation energy of the DV model is much higher than that of the DT model under Si-rich conditions. For the 6H-SiC(0001) surface, the ST model is energetically more favourable than the Tri-Ad model in the whole range of chemical potential of the surface Si atom. Therefore, we believe that the DT model and the ST model are more appropriate for the $(2\sqrt{3}\times2\sqrt{3})$ reconstructions on the surface of the 3C-SiC(111) island [2] and the 6H-SiC(0001) surface [4], respectively.

As mentioned above, the formation energies of the $(2\sqrt{3}\times2\sqrt{3})$ models do not depend on the polytypes of the SiC substrates. This implies that different structures of the DT and ST models for the $(2\sqrt{3}\times2\sqrt{3})$ reconstructions on the SiC surfaces are not caused by the 3C-SiC and the 6H-SiC substrate. We suggest, as Pollmann *et al* pointed out for the SiC(001)-c(4×2) reconstruction [1], that the structural difference of the $(2\sqrt{3}\times2\sqrt{3})$ reconstructions

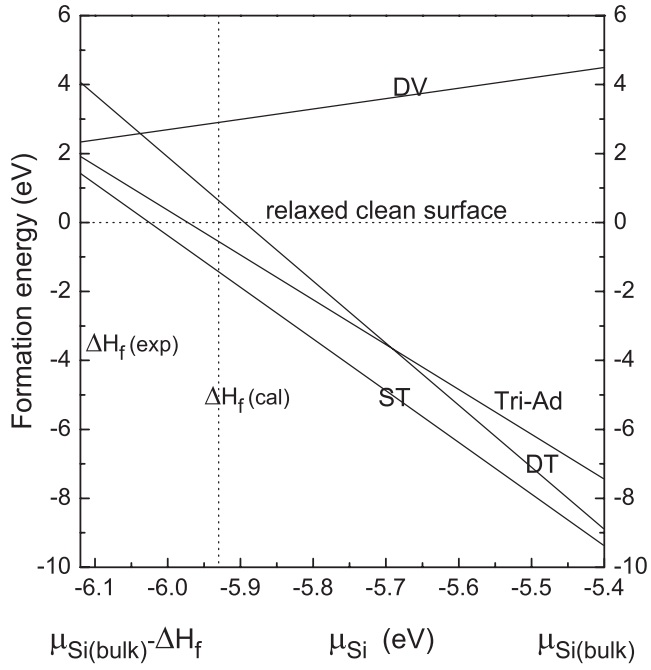

Figure 9. The formation energies per $(2\sqrt{3}\times 2\sqrt{3})$ cell of the DT, ST, Tri-Ad and DV models. The scale of the abscissa extends over the experimental value of $\Delta H_{\rm f}$ (exp) (0.72 eV) and the calculated value $\Delta H_{\rm f}$ (cal) is also marked.

in the above two experiments is caused by different preparation conditions such as annealing temperature and Si flux. In fact, the heat action of the SiC(111)-(7 × 7) surface with the fullerene molecules always forms a very Si-rich SiC surface [24–26], while annealing without Si flux would decrease the Si coverage of the surface [1]. As a result, two different structures of the $(2\sqrt{3} \times 2\sqrt{3})$ reconstructions with different Si coverages appeared on the SiC surface. Since the difference between the formation energies of the DT and ST models is only 0.5 eV per $(2\sqrt{3} \times 2\sqrt{3})$ cell, it is reasonable to believe that annealing the surface of the 6H-SiC(0001)-$(2\sqrt{3} \times 2\sqrt{3})$ ST model under a strong Si flux could transform it into the surface of the 6H-SiC(0001)-$(2\sqrt{3} \times 2\sqrt{3})$ DT model. As shown in figures 1 and 5, this transformation could occur after 3/12 monolayer Si atoms are adsorbed on the sites between atoms *e* and atoms *f* of the ST model.

4. Conclusions

In this work, we have proposed a double-trimer model and a single-trimer model for the $(2\sqrt{3} \times 2\sqrt{3})$R30° reconstructions observed on the surface of the 3C-SiC(111) island and the 6H-SiC(0001) surface, respectively. The calculations of the formation energies reveal that our proposed models are energetically more favourable than the previously reported DV and Tri-Ad models. The simulated STM images for these two models are in good agreement with the experimental observations. In the double-trimer model, Si atoms of the different trimers form buckled dimers. The dangling bonds on the dimers form π bonds, which results in a semiconducting surface. The single-trimer model also has a semiconducting surface, which is different from the metallic surface of the Tri-Ad model.

Acknowledgments

This work was supported by the National Natural Science Foundation of China (grant no 60176005), and the Foundation of National High Performance Computing Centre and Fudan High-End Computing Centre, Shanghai, China.

References

[1] Pollmann J and Krüger P 2004 *J. Phys.: Condens. Matter* **16** S1659 and the references therein
[2] Pascual J I, Gómez-Herrero J and Baró A M 1998 *Surf. Sci.* **397** L267
[3] Yang J, Wang X S, Zhai G J, Cue N and Wang X 2001 *Surf. Sci.* **476** 1
[4] Amy F, Soukiassian P and Brylinski C 2004 *Appl. Phys. Lett.* **85** 926
[5] Peng X, Wang X and Ye L 2002 *Surf. Sci.* **501** 125
[6] Starke U, Schardt J, Bernhardt J, Franke M, Reuter K, Wedler H, Heinz K, Furthmüller J, Käckell P and Bechstedt F 1998 *Phys. Rev. Lett.* **80** 758
[7] Li Y, Ye L and Wang X 2006 *Surf. Sci.* **600** 298
[8] Kulakov M A, Henn G and Bullemer B 1996 *Surf. Sci.* **346** 49
[9] Badziag P 1998 *Surf. Sci.* **402–404** 822
[10] Kresse G and Hafner J 1993 *Phys. Rev.* B **47** R558
Kresse G and Hafner J 1994 *Phys. Rev.* B **49** 14251
Kresse G and Furthmüller J 1996 *Comput. Mater. Sci.* **6** 15
Kresse G and Furthmüller J 1996 *Phys. Rev.* B **54** 11169
[11] Wang Y and Perdew J P 1991 *Phys. Rev.* B **44** 13298
[12] Vanderbilt D 1990 *Phys. Rev.* B **41** R7892
Kresse G 1996 *J. Phys.: Condens. Matter* **6** 5824
[13] Chadi D J 1979 *Phys. Rev. Lett.* **43** 43
[14] Yin M T and Cohen M L 1981 *Phys. Rev.* B **24** 2303
[15] Ramstad A, Brocks G and Kelly P J 1995 *Phys. Rev.* B **51** 14504
[16] Yokoyama T and Takayanagi K 2000 *Phys. Rev.* B **61** R5078
[17] Ono M, Kamoshida A, Matsuura N, Ishikawa E, Eguchi T and Hasegawa Y 2003 *Phys. Rev.* B **67** 201306
[18] Jones R O and Gunnarson O 1989 *Rev. Mod. Phys.* **61** 689
[19] Bardeen J 1961 *Phys. Rev. Lett.* **6** 57
[20] Tersoff J and Hamann D R 1985 *Phys. Rev.* B **31** 31805
[21] Qian G X, Martin R M and Chadi D J 1988 *Phys. Rev.* B **38** 7649
[22] Northrup J E and Froyen S 1993 *Phys. Rev. Lett.* **71** 2276
[23] Sabisch M, Krüger P and Pollmann J 1997 *Phys. Rev.* B **55** 10561
[24] Hamza A V, Balooch M and Moalem M 1994 *Surf. Sci.* **31** L1129
[25] Chen D, Workman R and Sarid D 1995 *Surf. Sci.* **334** 23
[26] Hu C W, Kasuya A, Suto S, Wawro A and Nishina Y 1996 *Appl. Phys. Lett.* **68** 1253